Neural correlates of illusory motion perception in *Drosophila*

John C. Tuthill[a,b], M. Eugenia Chiappe[a], and Michael B. Reiser[a,1]

[a]Janelia Farm Research Campus, Howard Hughes Medical Institute, Ashburn, VA 20147; and [b]Joint Janelia Farm Research Campus\University of Chicago Graduate Program, University of Chicago, Chicago, IL 60637

Edited by Chi-Hon Lee, National Institutes of Health, Bethesda, MD, and accepted by the Editorial Board April 19, 2011 (received for review January 5, 2011)

When the contrast of an image flickers as it moves, humans perceive an illusory reversal in the direction of motion. This classic illusion, called reverse-phi motion, has been well-characterized using psychophysics, and several models have been proposed to account for its effects. Here, we show that *Drosophila melanogaster* also respond behaviorally to the reverse-phi illusion and that the illusion is present in dendritic calcium signals of motion-sensitive neurons in the fly lobula plate. These results closely match the predictions of the predominant model of fly motion detection. However, high flicker rates cause an inversion of the reverse-phi behavioral response that is also present in calcium signals of lobula plate tangential cell dendrites but not predicted by the model. The fly's behavioral and neural responses to the reverse-phi illusion reveal unexpected interactions between motion and flicker signals in the fly visual system and suggest that a similar correlation-based mechanism underlies visual motion detection across the animal kingdom.

fly vision | *Drosophila* behavior | calcium imaging | visual illusion

Among visual organisms, the ability to detect motion is nearly universal. Animals as diverse as weevils (1) and wallabies (2) compute visual motion from time-varying patterns of brightness received by an array of photoreceptors. However, the mechanisms by which the visual system detects motion are not well-understood in any animal (3). Here, we use a visual illusion to probe the mechanisms of motion detection in the fly, *Drosophila melanogaster*.

Sequential flashes at neighboring spatial positions cause humans to perceive motion in the direction of the second flash, an effect called phi or apparent motion (4). A related phenomenon, reverse-phi motion, also relies on sequential luminance changes to evoke a motion percept (5); however, in the reverse-phi stimulus, the contrast polarity of the stimulus inverts as it moves, causing a reversal in the direction of perceived motion (Movie S1). For example, when a black random dot pattern turns to white as it moves right across a gray background, human subjects perceive left motion (6).

The reverse-phi effect is not a subtle illusion. Humans exhibit nearly equal sensitivity and comparable spatial and temporal tuning for standard and reverse-phi motion (7). Sensitivity to reverse-phi has also been shown for other vertebrates such as primates (8) and zebrafish (9). Directional responses to reverse-phi motion are present in cat striate cortex (10), the nucleus of the optic tract in the wallaby (2), and the middle temporal area (MT) of primate visual cortex (8, 11). These psychophysical and neurophysiological data suggest that sensitivity to reverse-phi motion may be a common feature of motion detection in the vertebrate visual system, and for this reason, reverse-phi has been an important tool for building models of visual motion detection (8, 12–16).

The prevailing simple model for motion detection in the fly is the Hassenstein–Reichardt elementary motion detector (H-R EMD), in which the intensity measured at one photoreceptor is temporally filtered and multiplied with a neighboring intensity signal (17). Columnar motion detection circuits compute local motion features across the fly eye, which are then integrated to produce global motion percepts (18). Anatomically, local motion computations are presumed to be implemented within columnar circuits of the lamina and medulla (19); local motion signals are then integrated by wide-field tangential cells in the lobula plate that encode global motion patterns (Fig. 1*A*) (20).

In this paper, we examine behavioral and physiological responses to reverse-phi motion as a test of this conceptual framework in a genetic model organism, *D. melanogaster*. We found that flies exhibit reverse-optomotor behavioral responses when presented with panoramic reverse-phi motion and that the dendrites of neurons in the fly lobula plate are also sensitive to this illusion. Experiments using combinations of motion and flicker stimuli revealed aspects of motion computation not explained by the EMD model, and we propose specific modifications to the EMD to explain these results.

Results

Responses to Panoramic Standard and Reverse-phi Motion. We studied visually guided behavior in tethered flies suspended in a virtual reality flight simulator, which allowed us to precisely control the fly's visual environment while monitoring her behavior with an optical wing-beat analyzer (Fig. 1*B*) (21). When faced with a rotating square-wave intensity stimulus, tethered flies attempt to turn in the direction of motion—a behavior known as the optomotor response (Fig. 1*D Top*) (22).

To determine whether flies perceive the reverse-phi illusion, we first compared optomotor steering behavior to standard and reverse-phi motion stimuli (Fig. 1*C*). The reverse-phi stimulus was similar to the standard stimulus, except that every other stripe alternated between bright and dark as it moved (Fig. 1*C* and Movie S1). Hence, this stimulus contained both motion and flicker components. Rotation of the reverse-phi stimulus evoked reverse-optomotor responses—flies steered against the direction of motion (Fig. 1*D Middle*)—showing that flies respond to the reverse-phi illusion with an inverted optomotor response. The reverse-optomotor response peaked at low stimulus velocities; at higher velocities, flies only transiently turned against the direction of stimulus motion followed by steering in the opposite direction. Reverse-phi responses were robust to large changes in the global structure of the stimulus. For example, standard and reverse-optomotor responses persisted even when the spatial extent of the stimulus was reduced to a narrow window (Fig. S1), and responses to translational (23, 24) standard and reverse-phi

Author contributions: J.C.T., M.E.C., and M.B.R. designed research; J.C.T., M.E.C., and M.B.R. performed research; J.C.T. and M.E.C. analyzed data; and J.C.T., M.E.C., and M.B.R. wrote the paper.

The authors declare no conflict of interest.

This article is a PNAS Direct Submission. C.-H.L. is a guest editor invited by the Editorial Board.

Freely available online through the PNAS open access option.

[1]To whom correspondence should be addressed. E-mail: reiserm@janelia.hhmi.org.

This article contains supporting information online at www.pnas.org/lookup/suppl/doi:10.1073/pnas.1100062108/-/DCSupplemental.

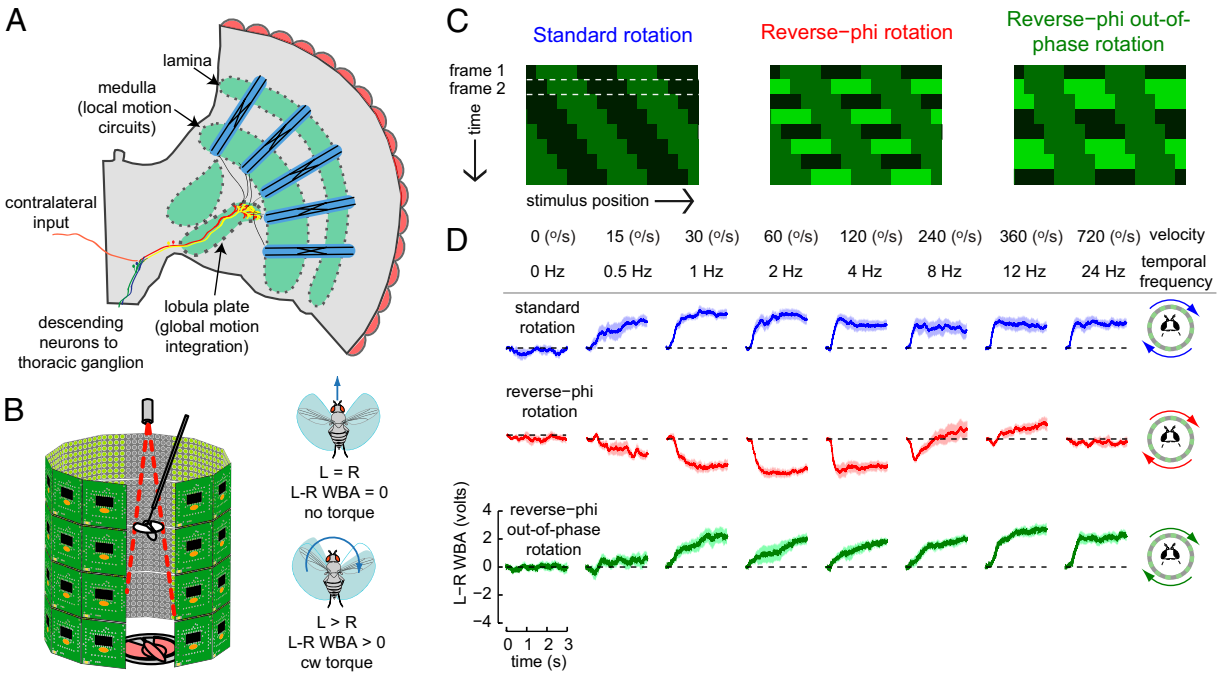

Fig. 1. Flies faced with panoramic reverse-phi motion exhibit reverse-optomotor responses. (*A*) A schematic model for fly motion vision consists of two stages: (*i*) local motion is computed by columnar circuits within the lamina and medulla, which is followed by (*ii*) global integration of local motion signals in the lobula plate tangential cells. The output of the LPTCs is thought to control optomotor behavior. (*B*) The fly is suspended within a virtual flight arena where the amplitude of each wing-beat is tracked by an optical detector. The difference between the two wing-beats (left minus right wing-beat amplitude) is proportional to yaw torque (24). For example, when the amplitude of the left wing-beat is greater than the right, the fly is attempting to steer to the right with clockwise torque. (*C*) Space–time depictions of motion stimuli used in rotation experiments—all three are square-wave patterns moving from the top left to the bottom right (Movie S1). (*D*) Mean turning behavior of 10 flies (±SEM) in response to open-loop rotation of standard (*Top*), reverse-phi (*Middle*), and reverse-phi out-of-phase (*Bottom*) square-wave gratings (λ = 30°). The speed of reverse-phi out-of-phase stimuli moved at one-half of the speed of the standard and reverse-phi stimuli, because motion occurred only in every second frame (the space–time plot in *C*). Flies were presented with motion in both directions (CW and CCW), but responses are combined and plotted for CW rotation (*SI Text* has a complete description of data treatment).

stimuli were similar to responses to rotation stimuli in directionality and temporal tuning (Fig. S2).

Although tethered flies do not exhibit directional turning responses to pure wide-field flicker stimuli, it is possible that adding flicker to a motion stimulus simply interferes with the standard optomotor response. To test whether adding flicker reverses optomotor behavior, we used a third stimulus that we call reverse-phi out of phase rotation. This stimulus was similar to the reverse-phi stimulus except that the flicker occurred out of phase with the discrete motion steps (Fig. 1*C* and Movie S1). When flicker was out of phase with motion, the reverse-phi illusion was abolished (Fig. 1*D Bottom*). This result confirms an important feature of fly motion detection—that it is strictly local in both space and time (17, 25). Although the discrete motion steps are generated by bars of alternating intensity, the flies respond as if they were presented with flicker-free standard motion.

Reverse-Optomotor Responses Are Largely Predicted by the EMD Model. In the H-R EMD model, the intensity measured at one input (nominally a photoreceptor) is delayed by a first-order low-pass filter and multiplied with a neighboring intensity signal (17); subtracting the output of the two mirror symmetrical arms of the EMD results in a directionally selective signal (Fig. 2*A*). Because of the multiplication stage of the EMD model, successive activation of neighboring subunits with signals of opposite polarity results in a negative output (17), suggesting a mechanism for the fly's sensitivity to reverse-phi motion (Fig. 2*A*).

To what extent are the behavioral responses to reverse-phi motion accounted for by local motion computation of H-R EMDs? To explicitly test this question, we constructed tuning curves comparing optomotor and reverse-optomotor behavior across spatial and temporal stimulus parameters with the tuning curves predicted by modeling. The amplitudes of rotation responses increased with stimulus velocity before decaying at the highest velocities tested (Fig. 2*B Left*). Notably, each curve, corresponding to one spatial period, peaks within a different range of stimulus velocities, but when plotted against temporal frequency (the ratio of angular velocity and spatial wavelength), the curves are clearly tuned to a common range of optimal temporal frequencies (4–16 Hz) across spatial periods (Fig. 2*B Inset*). In comparison, reverse-phi turning responses were of opposite sign and distinctly tuned to the velocity of the stimulus—they exhibit a velocity optimum centered at 30°/s across spatial periods (Fig. 2*B Right*) and are not tuned to temporal frequency (Fig. 2*B Inset*). The velocity dependence of the reverse-phi tuning curves suggests that reverse-optomotor responses are tuned to the flicker rate of the stimulus, which is constant across spatial frequencies. As was shown in Fig. 1*D*, the reverse-phi response inverts at higher velocities; the inversion is absent for the smallest spatial period in this time-averaged response and is quite prominent for the lower spatial period stimuli (Fig. 2*B*).

To compare fly behavior with the predictions of the H-R EMD model, we simulated the response of an EMD (with compound eye optics) to reverse-phi and standard motion stimuli identical to those used in our experiments (model details in *SI Text*). Although the EMD model predicts a temporal frequency optimum for standard rotation, for the reverse-phi stimuli, the model results exhibit a velocity optimum independent of spatial period (Fig. 2*C*). Varying the time constant of the EMD low-pass and

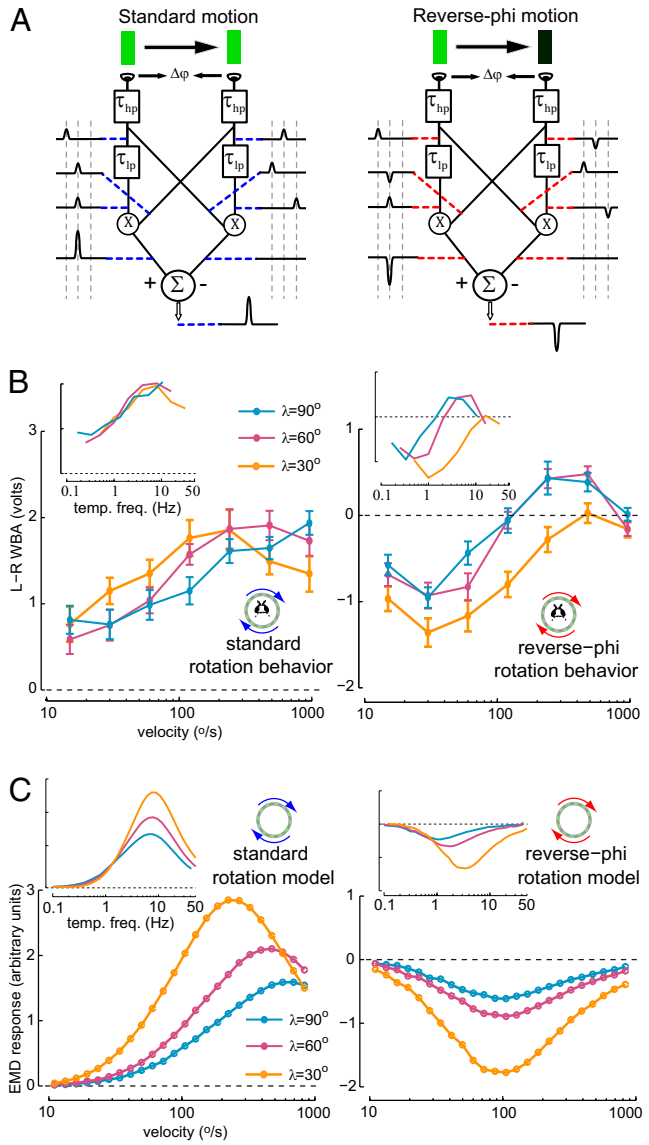

Fig. 2. The H-R EMD model of motion detection accounts for sensitivity to reverse-phi motion. (*A*) The H-R EMD requires two adjacent sampling units (e.g., photoreceptors) separated by a sampling base with distance Δϕ. Incoming luminance signals are high pass-filtered (τ_{hp}) before they are temporally delayed (τ_{lp}) and multiplied with the signal from the neighboring retinal sampling unit. The output signals of the two subunits are then subtracted (Σ). Standard motion in the EMD's preferred direction produces a positive output (38), whereas reverse-phi motion causes signals of opposite polarity to coincide at the multiplication stage, resulting in a negative output. (*B*) Behavioral tuning curves for standard and reverse-phi motion stimuli. Mean turning responses (±SEM; n = 10) to 3 s of standard (*Left*) or reverse-phi (*Right*) rotation. Stimulus velocity and spatial wavelength (λ) were varied across trials, and turning responses are shown as a function of both velocity and temporal frequency (*Inset*). Responses to standard motion exhibit temporal frequency tuning, whereas reverse-phi responses are velocity-tuned but feature an inversion at high speeds. (*C*) Modeled EMD responses to clockwise rotation are plotted as a function of both velocity and temporal frequency (*Inset*). For standard rotation, the model response is positive for a CW stimulus and exhibits a constant temporal frequency optimum across spatial wavelengths. For the reverse-phi stimulus, the model output is negative and tuned to the velocity of the stimulus.

high-pass filter time constants did not qualitatively affect these results (*SI Text* and Fig. S3). Overall, the EMD simulation captured most features of standard and reverse-optomotor flight behavior, and it provides evidence for a local correlation-based mechanism underlying perception of the reverse-phi illusion. However, the inversion of the reverse-phi response at higher motion rates is strikingly absent from the simulation results of the standard EMD model.

Responses of a Motion-Sensitive Neuron to Reverse-phi Motion. A group of large motion-sensitive neurons in the fly visual system, the lobula plate tangential cells (LPTCs), spatially integrates signals from an array of small-field local directionally selective neurons (18), forming receptive fields that match the complex patterns of global optic flow that a fly encounters during self-motion (20). Previous studies in blowflies have also shown that the spiking H1 neuron displays directional responses when the eye is stimulated locally (26–28). In one case, Egelhaaf and Borst (28) used apparent motion stimuli that consisted of sequential brightness changes of same and opposite polarity bars—discrete, local analogs of the standard and reverse-phi motion stimuli used in this study. To test whether responses to reverse-phi are present at the input level of the LPTCs, we optically recorded transient calcium signals from the LPTC dendrites, the site where integration of local EMDs is thought to occur (18, 20).

Within the LPTC network, the horizontal system (HS) neurons are required for optomotor behavior in blowflies (29, 30). Recently, the response properties of HS neurons have also been characterized in *Drosophila* (31–33) and found to be largely similar to the blowfly. Because HS neurons likely subserve the behaviors measured in our previous experiments, we chose to perform all imaging experiment in the horizontal system north (HSN) neuron. Because the gain and tuning of LPTCs depend on the behavioral state of the animal (31, 34), we performed all imaging experiments in behaving flies to ensure that even small neural signatures of the reverse-phi illusion could be observed (Fig. S4). We expressed the genetically encoded calcium indicator gCaMP3.0 (35) in HS neurons using the GAL4-UAS binary expression system (36) and imaged changes in fluorescence with two-photon microscopy while flies walked on an air-supported ball within an arena similar to that used in the flight behavior experiments (Fig. 3*A*) (32).

In agreement with previous work (31, 33), HSN in the left lobula plate (Fig. 3*B*) responded to standard motion in its preferred or counter clockwise (CCW) direction with an increase in calcium signal. There was no change in calcium signal if the standard motion stimulus was moving clockwise (CW) in the null direction of the left HSN (Fig. 3*C*). In contrast, a reverse-phi stimulus moving in the neuron's null direction (CW) evoked a larger calcium response than when the stimulus moved in the cell's preferred direction (CCW). When flicker was decoupled from motion in the reverse-phi out of phase stimulus, the neuron responded more strongly to a stimulus moving in its standard preferred direction (CCW). HSN also responded to a non-directional full-field flicker stimulus in agreement with previous electrophysiological results from blowfly LPTCs (27, 37). We attribute the weaker calcium responses to null direction reverse-phi and reverse-phi out of phase stimuli to the flicker components of these stimuli (see below).

We further investigated the reverse-phi effect in HSN by presenting the three motion stimuli at several velocities and wide-field flicker at several rates (Fig. 3*D*). We found strong qualitative agreement between the temporal frequency tuning curves that we obtained from imaging (Fig. 3*D Left*) and the results of behavior (Figs. 1 and 2) and the H-R EMD simulation (Fig. 2*C*). For example, flight behavior, EMD simulation, and HSN responses were tuned to higher temporal frequencies for standard motion than reverse-phi motion, although the absolute frequencies of maximum sensitivity were lower in the neuronal response—we attribute this to differences in speed tuning between walking and flying (31). When we compared the tuning curves obtained with the three stimuli containing flicker (CW reverse-phi, CCW

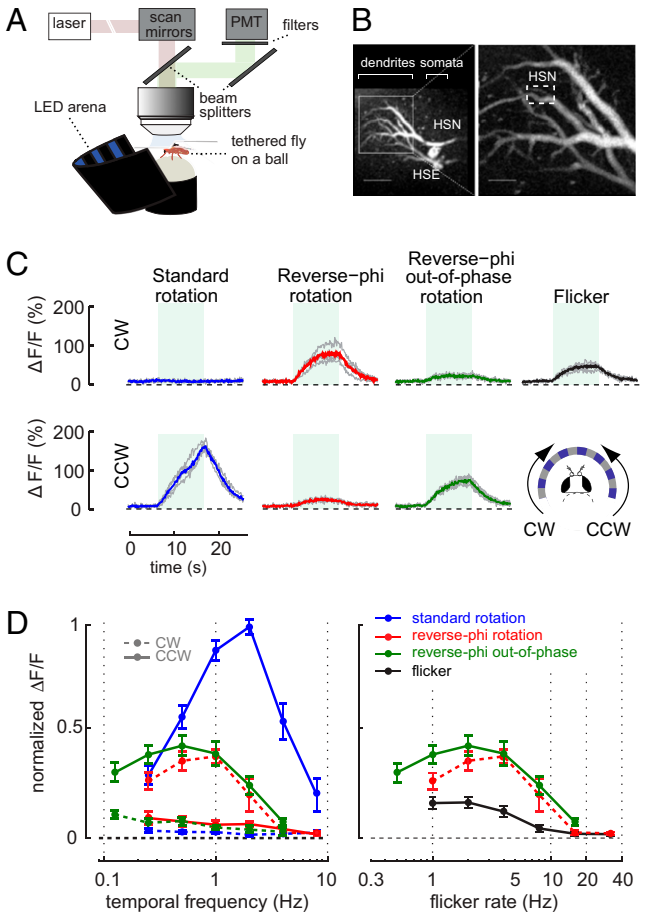

Fig. 3. The LPTC HSN responds to reverse-phi motion with inverted direction selectivity. (*A*) The experimental setup used to record calcium transients from LPTC dendrites consists of a tethered fly walking on an air-supported ball. (*B Left*) Low magnification of the left hemisphere of the fly brain (dorsal to the left and midline to the top) with horizontal system north (HSN) and equatorial (HSE) neurons labeled with gCaMP3.0. (Scale bar: 25 μm.) (*Right*) Higher magnification view of the dendritic arbors of the HS neurons showing the region of interest selected to analyze HSN responses to moving stimuli. (Scale bar: 7 μm.) (*C*) Example from a single fly of the HSN responses to visual motion stimuli updated at the same frame rate (corresponding to a temporal frequency of 1 Hz for standard motion; four to five repetitions each; individual trials are gray and the mean is depicted in the corresponding color: blue, standard rotation; red, reverse-phi; green, reverse-phi out of phase). The shaded region denotes the onset and duration of the visual stimulation. (*D*) Normalized HSN dendrite responses ($n = 9$ flies; mean $\Delta F/F$ ±SEM during the last 0.5 s of the stimulation) to motion (*Left*) and flicker-containing stimuli (*Right*). Flicker rates within the response range of the HSN neuron elicited mean responses that were significantly lower than those induced by either CW reverse-phi motion (*Right*; $P < 0.001$, *u* test with the sole exception of the lowest flicker rate tested, $P = 0.09$) or CCW reverse-phi out of phase ($P < 0.0005$, *u* test).

reverse-phi out of phase, and wide-field flicker), we found that flicker alone could not account for the observed responses to reverse-phi motion (Fig. 3*D Right*). Interestingly, responses to wide-field flicker were inhibited if motion was also present, which was revealed by comparing the responses to null direction movement of reverse-phi and reverse-phi out of phase stimuli with those obtained with wide-field flicker only (Fig. 3 *C* and *D*). Overall, the similarities between flight behavior and HSN responses show that the reverse-phi illusion is present at the level of the HSN dendrites, suggesting that small-field motion detectors underlie behavioral sensitivity to the reverse-phi illusion.

Temporal Deconstruction of the Reverse-phi Stimulus. To further explore interactions between motion and flicker, we deconstructed the reverse-phi stimulus into its individual components by independently varying the rates of contrast flicker and motion (Movie S2). In the absence of flicker, flies steered in the direction of stimulus motion (Fig. 4*A*, row 1). Reverse-optomotor responses were strongest when the flicker rate was equal to the rate of stimulus motion (Fig. 4*A*, red traces). In the three conditions with low flicker rates and high motion velocities, standard optomotor behavior persisted (denoted with blue asterisks), indicating that the illusion is abolished when the standard motion component occurs much more frequently than the reverse-phi steps. Surprisingly, flies also turned against the direction of stimulus motion when the flicker occurred in every other motion step—that is, when the stimulus consisted of equal parts reverse-phi and standard motion (red asterisks). This behavior cannot be explained as the linear combination of the responses to the two stimuli, because when presented in isolation the steering responses to standard motion are larger in amplitude. It is also not captured by the EMD model (the green lines in Fig. 4*A* denote predictions of the EMD). Interestingly, in the three cases (denoted with black asterisks) where the combined stimulus flickers at an integer multiple of the motion step rate, the reverse-phi response is abolished, although flicker always accompanies the motion step. At the higher flicker rates, flies often steered transiently in the direction of the reverse-phi stimulus followed by a corrective steering response in the opposite direction (Fig. 1*D*), presumably reflecting an adaptive mechanism that is enhanced by flicker. We call this phenomenon the flicker-mediated inversion.

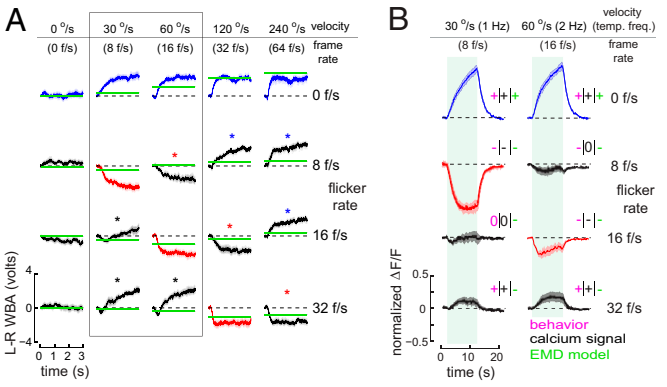

Fig. 4. Independently varying contrast and flicker rates reveals local motion computations not predicted by the EMD model. (*A*) Mean turning responses (±SEM; $n = 10$ flies) to reverse-phi rotating stimuli in which the velocity and rate of contrast reversal were controlled independently (Movie S2). Rotation occurred at one of five velocities, and the contrast of the stimulus was inverted at one of four flicker rates. Blue traces indicate standard motion (no flicker), and red traces indicate reverse-phi (flicker rate is equal to motion frame rate). Blue asterisks denote conditions with low flicker rates and high motion frame rates, black asterisks indicate when the stimulus flickers at an integer multiple of the motion frame rate, and red asterisks indicate when the motion frame rate is two times the flicker rate. Green lines represent the steady-state output of an elementary motion detector simulation (same model parameters as in Fig. 2*C*) to each visual stimulus. (*B*) Normalized HSN dendrite responses (±SEM; $n = 6$ flies) to reverse-phi motion stimuli in which the rate of contrast reversal was independently varied (identical stimuli as in columns 2 and 3 of *A*; traces color coded as in *A*). To facilitate comparison with the behavioral results, each time series is plotted as CCW responses minus CW responses (calculated from the individual traces in Fig. S5). *Insets* on the right of each trace show whether HSN calcium transients (black), fly behavior (magenta), and EMD model prediction (green) are significantly greater than (+), less than (–), or not different (0) from zero, measured as the normalized mean response to the same stimulus ($P < 0.1$, one-tailed *t* test).

Where does the flicker-mediated inversion originate? To test whether it is present in the output of the elementary motion detection circuitry, we performed a subset of the same experimental conditions while imaging calcium transients from the HSN cell dendrites (Fig. 4*B*). As expected, we observed robust calcium responses to standard motion in the absence of flicker (blue traces), and an opposite direction response when the flicker and motion rates were equal (red traces). In cases where we observed the flicker-mediated inversion in flight behavior (i.e., when the flicker rate was greater than the rate of stimulus motion), we found that calcium accumulation in the HSN dendrites also reflected this inversion (Fig. 4*B* and Fig. S5). These data agree with our behavioral results but contradict the predictions of the standard EMD model (Fig. 4*B Inset*). They also show an unexpected interaction between flicker and motion detection in the fly visual system.

Discussion

Our results show that *D. melanogaster* exhibit reverse-optomotor responses when faced with reverse-phi motion (Fig. 1 and Figs. S1 and S2) (that is, they perceive the illusion in much the same way as do vertebrates). HSN dendrites in the lobula plate of walking flies also respond to reverse-phi stimuli with reverse direction selectivity (Fig. 3). Behavioral (Figs. 1 and 2), physiological (Fig. 3), and modeling (Fig. 2) data suggest that the reverse-phi illusion is computed at the level of local motion detection circuits, the outputs of which are then integrated at the dendrites of the LPTCs. However, we also identified a flicker-mediated inversion of the reverse-phi illusion (Fig. 4*A*) that is not explained by the classical EMD model. Calcium imaging in the HSN dendrites suggests that this inversion occurs presynaptic to the LPTCs (Fig. 4*B*).

EMD Model Captures Many Features of Reverse-phi Sensitivity. Over 50 years ago, Hassenstein and Reichardt used an analog of the reverse-phi stimulus to describe and model motion detection in a snout beetle, *Chlorophanus* (17). They observed that alternately presenting two adjacent bars of the same polarity (ON-ON) caused the beetles to turn in one direction, but bars of opposite polarity (ON-OFF) elicited a turn in the opposite direction. This led them to conclude that motion detection involved multiplication of neighboring luminance signals and resulted in the formulation of the EMD model, which has since been used to describe motion detection in many animals, including humans (38, 39).

The EMD and other closely related models based on spatiotemporal correlation, such as the Barlow and Levick (40) and motion energy models (14), are inherently susceptible to the reverse-phi illusion (Fig. 2*A*) (7, 13). In contrast, the primary alternative class of models for motion detection, based on the so-called gradient detector (41), will not detect any directional motion in response to a reverse-phi stimulus without substantial modification (12). Although the neural implementation of spatiotemporal correlation in the fly visual system is currently unknown, the EMD model serves as a useful comparison for our behavioral and physiological data.

A nonintuitive prediction of the EMD model is that responses to reverse-phi motion will peak at a particular velocity. To understand this, it is useful to consider the discrete events that give rise to motion signals. In the case of standard motion, these events are generated by the motion of edges (light to dark and dark to light transitions) whose arrival rate is determined by the temporal frequency, defined as the ratio of the angular velocity and spatial period of the stimulus. Above a peak temporal frequency set by the EMD low-pass filter time constant, response amplitudes are attenuated, producing the characteristic tuning curves shown in Fig. 2*C*. By contrast, the discrete motion events induced by a reverse-phi stimulus are generated by flickering edges that occur at a rate set by the stimulus velocity, independent of spatial frequency. Therefore, in the reverse-phi stimulus, the flicker rate serves the same role in specifying the peak response as the temporal frequency does for standard motion stimuli. In agreement with this prediction, behavioral responses to reverse-phi motion exhibit a pronounced velocity optimum, whereas responses to standard motion peak at a particular temporal frequency (Fig. 2*B*). Overall, the EMD model captures several key features of the data in Figs. 1–3.

Features Not Captured by the EMD Model. By combining motion and flicker stimuli, we identified a flicker-mediated inversion of the flies' optomotor response that is not predicted by the canonical EMD model. Under open-loop conditions, the optomotor steering response of the fly saturates rapidly (Fig. 1D and Fig. S1). However, when presented with reverse-phi stimuli, fly behavioral responses do not immediately saturate and adaptation occurs more rapidly, particularly at high flicker rates (Figs. 1*D* and 4*A*). In some cases, rapid adaption leads to a complete inversion of the reverse-optomotor response. This flicker-mediated inversion is apparent in fly optomotor responses to high velocity reverse-phi stimuli (Fig. 2*B*) or when the flicker rate exceeds the rate of stimulus motion (Fig. 4). Considering the striking agreement between the behavioral inversion and the calcium signals of the HSN dendrites (Fig. 4), it is clear that this rapid adaptation is present in the LPTC inputs and may be either upstream of local motion detection or an intimate and currently enigmatic feature of fly motion detection.

If the standard EMD cannot fully account for the fly's responses to combined motion and flicker stimuli, is there an alternative model that can? One possible explanation for the inversion is that temporal aliasing occurs in the motion detector at high flicker rates. For example, an EMD implemented with a temporal delay line, rather than a first-order low-pass filter, would produce inverted output values at some range of high flicker rates (Fig. S6). Inhibitory interneurons in the fly visual system (42) could execute such a fixed delay, as in the closely related Barlow and Levick model (13, 40).

Another feature seen in our data (Fig. 3*D*) and previous studies (26, 27) is the weak flicker sensitivity of the LPTC neurons. One potential explanation for this phenomenon is that motion detection circuits are not perfectly balanced, and there is evidence that LPTCs receive antagonistic signals from asymmetric EMDs with opposite preferred directions (26). Therefore, a model that accounts for both HSN flicker sensitivity and the flicker-mediated inversion is an elaborated EMD that includes asymmetric summation of motion signals and temporal aliasing because of a discrete temporal delay in the motion detector (Fig. S6). We presume that the adaptive time course of the behavioral responses (Figs. 1 and 4) is because of temporal adaptation in premotion circuits within the lamina and medulla. More complex models consisting of identified neuron types and biophysically realistic processing (13, 19) may prove useful in elucidating the contribution of adaptation to reverse-phi perception and motion computation.

Reverse-phi Motion as a Circuit-Breaking Tool. A powerful approach for studying the properties of visual circuits is reverse correlation-based system identification (43). However, motion circuits present a particular challenge, because motion detection relies on nonlinear interactions and structured spatiotemporal correlations. A primary motivation for studying visual illusions like reverse-phi is to identify behavioral and neural phenomena not resolvable with standard reverse-correlation techniques. As a complementary approach, the reverse-phi illusion promises to be an important tool for dissecting the neural circuitry that underlies motion detection. The reason for performing these studies in *Drosophila* is that the molecular genetic toolkit available in flies enables the identification and manipulation of motion circuits (44). For example, recent data suggest that signals are rectified into ON and OFF pathways

early in the motion pathway (45). One might predict that flies, like humans (15), are not equally sensitive to ON and OFF motion signals. Selectively silencing components of ON or OFF pathways might specifically disrupt sensitivity to reverse-phi motion.

Nearly a century ago, Cajal and Sanchez (46) speculated about the remarkably high degree of anatomical similarity between the peripheral visual systems of flies and vertebrates. We now know there are also striking genetic and developmental commonalities that support a common evolutionary origin (47). Despite 500 million years of evolution, fly and human eyes are also likely performing many of the same neural computations. Many visual illusions are perceived by both humans and insects (48), suggesting that similar neural mechanisms underlie visual processing across the animal kingdom. A further test of this analogy would be to look in humans for the surprising features of reverse-phi perception that we identify in this study. Sensitivity to both spatiotemporal correlations (standard motion signals) and anticorrelations (reverse-phi motion) may be part of a common strategy to average out noisy fluctuations in visual inputs, thus allowing movement detection circuits to be maximally sensitive to the most relevant and persistent motion signals in the environment.

Methods

For the tethered flight experiments, *D. melanogaster* from our laboratory culture were tethered to a tungsten wire with UV-cured glue and placed within an electronic visual flight simulator that presents stimuli with a linear intensity scale from 0 to 72 cdm^{-2} (21).The amplitude and frequency of the fly's wing-beats were monitored with an optical wing-beat analyzer. Further details are included in *SI Text*.

For two-photon imaging experiments, female flies expressing the genetically encoded calcium indicator GCaMP3.0 in HS neurons (using the *R27B03-GAL4* driver from the Rubin laboratory) were mounted in a custom holder in which the animal's legs were free to move on an air-supported ball. We imaged from the HSN dendrites of the left lobula plate using a custom-built two-photon microscope (Fig. 3*A*). Details of the preparations are described in *SI Text*, and experimental details are provided at http://www.flyfizz.org.

We modeled the local circuit of the *Drosophila* motion detection system as one H-R EMD beneath simple compound eye optics. Our EMD implementation was based on the modifications proposed to capture most of the related experimental phenomena: the classic model with first-order low-pass filter (τ = 20 ms; selected to match the temporal frequency optimum of 8 Hz) (Fig. 2) and a high-pass filter in the input lines to account for neural adaptation (τ = 200 ms; details in *SI Text*).

ACKNOWLEDGMENTS. We thank the Janelia Fly Core for help with fly care; Johannes Seelig for technical assistance; and Martin Lankheet, Vivek Jayaraman, Bart Borghuis, Gabe Murphy, and Aljoscha Nern for thoughtful comments on the work. We are grateful to Mitya Chklovskii and Arjun Bharioke for proposing the temporal aliasing effect in Fig. S6 and Simon Laughlin for suggesting the noise-averaging hypothesis. We thank Melina Hale for hosting early iterations of these experiments in her laboratory and Kevin Moses for supporting J.C.T. as a Janelia Graduate Scholar. This research was funded by the Howard Hughes Medical Institute.

1. Hassenstein VB, Reichardt W (1956) System theoretical analysis of time, sequence and sign analysis of the motion perception of the snout-beetle *Chlorophanus*. *Z Naturforsch* 11b:513–524.
2. Ibbotson MR, Clifford CW (2001) Interactions between ON and OFF signals in directional motion detectors feeding the NOT of the wallaby. *J Neurophysiol* 86:997–1005.
3. Clifford CW, Ibbotson MR (2002) Fundamental mechanisms of visual motion detection: Models, cells and functions. *Prog Neurobiol* 68:409–437.
4. Exner S (1875) Experimental investigation of the simplest mental processes. *Pflügers Arch* 11:403–432.
5. Anstis SM, Rogers BJ (1975) Illusory reversal of visual depth and movement during changes of contrast. *Vision Res* 15:957–961.
6. Sato T (1989) Reversed apparent motion with random dot patterns. *Vision Res* 29: 1749–1758.
7. Bours RJ, Kroes MC, Lankheet MJ (2009) Sensitivity for reverse-phi motion. *Vision Res* 49:1–9.
8. Krekelberg B, Albright TD (2005) Motion mechanisms in macaque MT. *J Neurophysiol* 93:2908–2921.
9. Orger MB, Smear MC, Anstis SM, Baier H (2000) Perception of Fourier and non-Fourier motion by larval zebrafish. *Nat Neurosci* 3:1128–1133.
10. Emerson RC, Citron MC, Vaughn WJ, Klein SA (1987) Nonlinear directionally selective subunits in complex cells of cat striate cortex. *J Neurophysiol* 58:33–65.
11. Livingstone MS, Pack CC, Born RT (2001) Two-dimensional substructure of MT receptive fields. *Neuron* 30:781–793.
12. Johnston A, Clifford CW (1995) A unified account of three apparent motion illusions. *Vision Res* 35:1109–1123.
13. Mo CH, Koch C (2003) Modeling reverse-phi motion-selective neurons in cortex: Double synaptic-veto mechanism. *Neural Comput* 15:735–759.
14. Adelson EH, Bergen JR (1985) Spatiotemporal energy models for the perception of motion. *J Opt Soc Am A* 2:284–299.
15. Wehrhahn C, Rapf D (1992) ON- and OFF-pathways form separate neural substrates for motion perception: Psychophysical evidence. *J Neurosci* 12:2247–2250.
16. Shioiri S, Cavanagh P (1990) ISI produces reverse apparent motion. *Vision Res* 30:757–768.
17. Reichardt W (1961) Autocorrelation, a principle for the evaluation of sensory information by the central nervous system. *Sensory Communication*, ed Rosenblith WA (Wiley, New York), pp 303–317.
18. Single S, Borst A (1998) Dendritic integration and its role in computing image velocity. *Science* 281:1848–1850.
19. Higgins CM, Douglass JK, Strausfeld NJ (2004) The computational basis of an identified neuronal circuit for elementary motion detection in dipterous insects. *Vis Neurosci* 21:567–586.
20. Borst A, Haag J, Reiff DF (2010) Fly motion vision. *Annu Rev Neurosci* 33:49–70.
21. Reiser MB, Dickinson MH (2008) A modular display system for insect behavioral neuroscience. *J Neurosci Methods* 167:127–139.
22. Götz KG (1964) Optomoter studies of the visual system of several eye mutants of the fruit fly *Drosophila*. *Kybernetik* 2:77–92.
23. Duistermars BJ, Chow DM, Condro M, Frye MA (2007) The spatial, temporal and contrast properties of expansion and rotation flight optomotor responses in *Drosophila*. *J Exp Biol* 210:3218–3227.
24. Tammero LF, Frye MA, Dickinson MH (2004) Spatial organization of visuomotor reflexes in *Drosophila*. *J Exp Biol* 207:113–122.
25. Buchner E (1976) Elementary movement detectors in an insect visual system. *Biol Cybern* 24:85–101.
26. Franceschini N, Riehle A, Le Nestour A (1989) Directionally selective motion detection by insect neurons. *Facets of Vision*, eds Stavenga DG, Hardie RC (Springer, Berlin), pp 361–390.
27. Egelhaaf M, Borst A, Reichardt W (1989) Computational structure of a biological motion-detection system as revealed by local detector analysis in the fly's nervous system. *J Opt Soc Am A* 6:1070–1087.
28. Egelhaaf M, Borst A (1992) Are there separate ON and OFF channels in fly motion vision? *Vis Neurosci* 8:151–164.
29. Hausen K, Wehrhahn C (1983) Microsurgical lesion of horizontal cells changes optomotor yaw responses in the blowfly *Calliphora erythrocephala*. *Proc R Soc Lond B* 219:211–216.
30. Geiger G, Nässel DR (1981) Visual orientation behaviour of flies after selective laser beam ablation of interneurones. *Nature* 293:398–399.
31. Chiappe ME, Seelig JD, Reiser MB, Jayaraman V (2010) Walking modulates speed sensitivity in *Drosophila* motion vision. *Curr Biol* 20:1470–1475.
32. Seelig JD, et al. (2010) Two-photon calcium imaging from head-fixed *Drosophila* during optomotor walking behavior. *Nat Methods* 7:535–540.
33. Schnell B, et al. (2010) Processing of horizontal optic flow in three visual interneurons of the *Drosophila* brain. *J Neurophysiol* 103:1646–1657.
34. Maimon G, Straw AD, Dickinson MH (2010) Active flight increases the gain of visual motion processing in *Drosophila*. *Nat Neurosci* 13:393–399.
35. Tian L, et al. (2009) Imaging neural activity in worms, flies and mice with improved GCaMP calcium indicators. *Nat Methods* 6:875–881.
36. Brand AH, Perrimon N (1993) Targeted gene expression as a means of altering cell fates and generating dominant phenotypes. *Development* 118:401–415.
37. Srinivasan M, Dvorak DR (1980) Spatial processing of visual information in the movement-detecting pathway of the fly. *J Comp Physiol A* 140:1–23.
38. Borst A, Egelhaaf M (1989) Principles of visual motion detection. *Trends Neurosci* 12: 297–306.
39. van Santen JP, Sperling G (1985) Elaborated Reichardt detectors. *J Opt Soc Am A* 2:300–321.
40. Barlow HB, Levick WR (1965) The mechanism of directionally selective units in rabbit's retina. *J Physiol* 178:477–504.
41. Srinivasan MV (1990) Generalized gradient schemes for the measurement of two-dimensional image motion. *Biol Cybern* 63:421–431.
42. Sinakevitch I, Strausfeld NJ (2004) Chemical neuroanatomy of the fly's movement detection pathway. *J Comp Neurol* 468:6–23.
43. Marmarelis PZ, McCann GD (1973) Development and application of white-noise modeling techniques for studies of insect visual nervous system. *Kybernetik* 12:74–89.
44. Rister J, et al. (2007) Dissection of the peripheral motion channel in the visual system of *Drosophila* melanogaster. *Neuron* 56:155–170.
45. Joesch M, Schnell B, Raghu SV, Reiff DF, Borst A (2010) ON and OFF pathways in *Drosophila* motion vision. *Nature* 468:300–304.
46. Cajal SR, Sanchez D (1915) Contributions to the understanding of nervous systems of insects. *Trab Lab Invest Biol* 13:1–167.
47. Sanes JR, Zipursky SL (2010) Design principles of insect and vertebrate visual systems. *Neuron* 66:15–36.
48. Srinivasan M (1993) Even insects experience visual illusions. *Curr Sci* 64:649–655.